Molecular Therapy
Nucleic Acids
Original Article

Induced-Decay of Glycine Decarboxylase Transcripts as an Anticancer Therapeutic Strategy for Non-Small-Cell Lung Carcinoma

Jing Lin,[1,2] Jia Hui Jane Lee,[3] Kathirvel Paramasivam,[4] Elina Pathak,[3] Zhenxun Wang,[3] Zacharias Aloysius Dwi Pramono,[5] Bing Lim,[3] Keng Boon Wee,[1,2] and Uttam Surana[4,6,7]

[1]Bioinformatics Institute, A*STAR, 30 Biopolis Street, Singapore 138671, Singapore; [2]Institute of High Performance Computing, A*STAR, 1 Fusionopolis Way, Singapore 138632, Singapore; [3]Genome Institute of Singapore, A*STAR, 60 Biopolis Street, Singapore 138672, Singapore; [4]Department of Pharmacology, National University of Singapore, 16 Medical Drive, Singapore 117660, Singapore; [5]Department of Research, National Skin Centre, 1 Mandalay Road, Singapore 308205, Singapore; [6]Bioprocessing Technology Institute, A*STAR, 20 Biopolis Way, Singapore 138668, Singapore; [7]Institute of Molecular and Cellular Biology, A*STAR, 61 Biopolis Drive, Singapore 138673, Singapore

Self-renewing tumor-initiating cells (TICs) are thought to be responsible for tumor recurrence and chemo-resistance. Glycine decarboxylase, encoded by the *GLDC* gene, is reported to be overexpressed in TIC-enriched primary non-small-cell lung carcinoma (NSCLC). GLDC is a component of the mitochondrial glycine cleavage system, and its high expression is required for growth and tumorigenic capacity. Currently, there are no therapeutic agents against GLDC. As a therapeutic strategy, we have designed and tested splicing-modulating steric hindrance antisense oligonucleotides (shAONs) that efficiently induce exon skipping (half maximal inhibitory concentration [IC_{50}] at 3.5–7 nM), disrupt the open reading frame (ORF) of GLDC transcript (predisposing it for nonsense-mediated decay), halt cell proliferation, and prevent colony formation in both A549 cells and TIC-enriched NSCLC tumor sphere cells (TS32). One candidate shAON causes 60% inhibition of tumor growth in mice transplanted with TS32. Thus, our shAONs candidates can effectively inhibit the expression of NSCLC-associated metabolic enzyme GLDC and may have promising therapeutic implications.

INTRODUCTION

A growing body of evidence suggests that tumors are driven by a subpopulation of self-renewing and evolving tumor-initiating cells (TICs; also known as cancer stem cells),[1–3] which play a critical role in tumor recurrence and resistance to chemotherapeutic agents. The initiation and maintenance of tumor growth[4,5] requires dysregulation of tumor suppressor and proto-oncogene signaling pathways, as well as remodeling of the intracellular metabolic fluxes to meet the increased bioenergetics and metabolites requirements.

Glycine decarboxylase, also known as glycine dehydrogenase or the P protein of the glycine cleavage system, was reported to be overexpressed in TIC-enriched primary non-small-cell lung carcinoma (NSCLC).[6] Encoded by the *GLDC* gene in humans, it functions in the metabolism of the amino acid glycine. In addition to GLDC (P protein), the glycine cleavage system includes three other proteins, namely, aminomethyltransferase (T protein), lipoamide dehydrogenase (L protein), and lipoyl-carrier protein (H protein). Both the growth and tumorigenesis capacity of TICs were found to be dependent on the high level of GLDC expression.[6] In normal cells, GLDC overexpression increases glycine-serine metabolism and nucleotide synthesis to promote cell proliferation and their transformation to cancer cells. The oncogenic effect of aberrant GLDC upregulation is corroborated by the clinical observations that high GLDC expression level is associated with higher mortality and poor survival rates in NSCLC and other cancer patients.[7–9] The observation that knockdown of GLDC expression in non-transformed cells does not affect cell viability[6] further suggests the therapeutic relevance of GLDC, because GLDC as a target may have a wide therapeutic index. Together, these findings underscore GLDC as a potential therapeutic target for NSCLC.

Although small molecules have been successfully deployed as therapeutic agents in the clinics, a large proportion of disease-relevant proteins of therapeutic value may not be amenable for inhibition by small molecules.[10–12] RNA-binding antisense oligonucleotides, however, can significantly expand the target space in the human genome. The antisense nucleotides bind to specific RNAs by Watson-Crick base-pairing and can be classified by their mechanistic mode of action into three common groups: gapmers, siRNAs, and steric hindrance antisense oligonucleotides (shAONs).[13] shAON (a single strand of chemically modified RNA bases that is resistant to RNase-H) is designed to compete with the RNA-binding proteins

Received 23 January 2017; accepted 3 October 2017;
https://doi.org/10.1016/j.omtn.2017.10.001.

Correspondence: Keng Boon Wee, Institute of High Performance Computing, A*STAR, 1 Fusionopolis Way, Singapore 138632, Singapore.
E-mail: weekb@ihpc.a-star.edu.sg
Correspondence: Uttam Surana, Institute of Molecular and Cellular Biology, A*STAR, 61 Biopolis Drive, Singapore 138673, Singapore.
E-mail: mcbucs@imcb.a-star.edu.sg

for binding to a nascent or mature mRNA and to modulate post-transcriptional processing. Unlike gapmers and siRNAs, effecting steric hindrance is the primary function of an shAON. Hence, every base and backbone linkage can be custom-modified chemically to enhance shAONs' in vivo stability, binding specificity, and resistance to endonucleases without loss of efficacy.[14–18] By sterically blocking specific RNA-binding proteins from their binding sites, an shAON can cause modulation of splicing leading to restoration and/or upregulation[19–23] and/or suppression[24,25] of protein production or isoform-switching.[26,27] Of particular clinical relevance is the demonstration that intranasal inhalation is an efficient vehicle for the delivery of antisense oligonucleotides to the respiratory tract and lungs in animal studies.[28–30]

In this study, shAONs were designed to induce exclusion of a specific exon in GLDC nascent transcripts to disrupt their codon reading frame. The aberrantly spliced transcripts are subsequently targeted for degradation via the endogenous nonsense-mediated decay pathway[31] to dramatically reduce protein expression. Three efficacious candidates were identified with half maximal inhibitory concentration (IC_{50}) at 3.5–7 nM in inducing specific exon exclusion and with IC_{50} < 10 nM in downregulating GLDC protein. Notably, the IC_{90} attained by the most efficient candidate is 20 nM in exon exclusion and <10 nM for protein downregulation. Each candidate inhibited the proliferation of both A549 and primary NSCLC tumor spheres (TS32) enriched with TICs, but did not significantly affect non-cancer MRC5 and HLF cells. In mice implanted with primary NSCLC tumor spheres enriched with TICs, post-engraftment intraperitoneal injections of the most efficient shAON resulted in a statistically significant 60% inhibition of tumor growth as compared to a control shAON. Together, these results suggest that our candidate shAONs are effective in downregulating the GLDC protein, and thus may have important therapeutic implications.

RESULTS

shAON Candidates to Induce Exclusion of a Specific GLDC Exon

shAONs were designed to induce specific exclusion or skipping of an out-of-frame exon in GLDC nascent transcripts for the purpose of generating premature termination codons (PTCs). As shown in Figure 1A, exclusion of any one of the 14 exons will generate multiple PTCs downstream, which predispose the resultant transcript for nonsense-mediated decay (NMD) or as a translation template for a truncated protein. Exons 7, 8, 13, 15, and 16 were each selected as a target exon for their propensity for shAON-induced skipping by their amenable secondary structures for shAON binding and the presence of splice regulatory motifs (as described below), and for the likelihood to activate NMD. 20 novel shAONs each targeting an exon (Table 1) were designed with a rational approach. In brief, more than 40,000 local secondary structures of a target exon and its flanking introns were used to identify RNA sites that are co-transcriptionally accessible for shAON binding.[32,33] The sites that contain putative splicing enhancer motifs[34] were selected as shAON target sites, thus eliminating the need to block the flanking splice sites of a target exon.

Because GLDC is overexpressed in A549 human lung adenocarcinoma epithelial cells (Figure S1A), it is an appropriate system to validate the shAONs. shAONs were first tested for their efficacy to induce specific exon skipping. For each validation experiment, A549 cells were transfected with 100 nM shAON, followed by the addition of 100 μg/mL cycloheximide at 5 hr post-transfection. By arresting protein synthesis, cycloheximide prevents the first round of translation of the transcripts lacking the skipped exon (hereon referred to as "skipped transcripts"), essential for the initiation of NMD. The exon-skipping efficiency of shAONs was determined by PCR amplification of the region covering the target exon 24 hr post-transfection, followed by densitometry analysis of the PCR products. The skipping efficiency is expressed as the percentage of amplicons with exon skipping relative to the total amplicons. Agarose gel electrophoresis of the PCR products was used to estimate specific exon skipping and the corresponding efficiency for each shAON (Figures 1B and 1C). The specificity of the exon skipping was confirmed by sequencing of the band corresponds to the skipped transcript excised from agarose gel (Figure 1D). 12 shAONs each targeting exons 7, 8, 13, or 16 were found to be effective and specific with the exception of two exon 8-targeting shAONs causing co-skipping of exon 7 in <20% of the total skipped transcripts. shAONs 7C, 7D, and 8D targeting exons 7 or 8 were the most efficient, inducing exon skipping in more than 80% of the transcripts. The extent to which the skipped transcripts were degraded by NMD was estimated by shAON transfection under the same conditions as above but in the absence of cycloheximide. Comparison between the skipping efficiency in the two experimental conditions indicates that cycloheximide protects the skipped transcript from NMD, because there is a higher proportion of skipped transcript in cycloheximide-treated samples (Figure S1B).

Dose Responses for the Three High-Efficiency shAONs

Exon-skipping efficiencies for the most efficient shAONs 7C, 7D, and 8D were determined at different transfection concentrations. Measured using PCR followed by densitometry (Figure 2A), the IC_{50} for these three shAONs ranges from 3.5 to 7 nM. Both 7C and 7D achieved higher than 90% exon skipping within the range of shAON concentrations tested, with 7C attaining IC_{90} at 20 nM. The high exon-skipping efficiency induced by shAONs 7C, 7D and 8D was confirmed by real-time qPCR (Figure S1C). To study the turnover rate of the skipped transcripts, we performed time-course experiments (up to 144 hr post-transfection of 7C, 7D, or 8D at 10 nM). The rate at which the skipped transcripts were cleared approximates first-order kinetics with a half-life of ~48 hr (Figure 2B). We performed real-time qPCR to measure the effect of the three selected shAONs in downregulating GLDC mRNA transcript in A549 cells. Compared with the cells transfected with the scrambled (control) shAON, the real-time qPCR analysis showed >70% downregulation of GLDC full-length transcript 24 hr after transfection with 10 nM 7C or 7D. 72 hr after transfection, both 7C and 7D could still induce >30% downregulation. The rate of downregulation induced by shAON 8D was lower compared with 7C and 7D. This may be because of the co-skipping of exon 7, possibly leading to codon reading frame restoration.

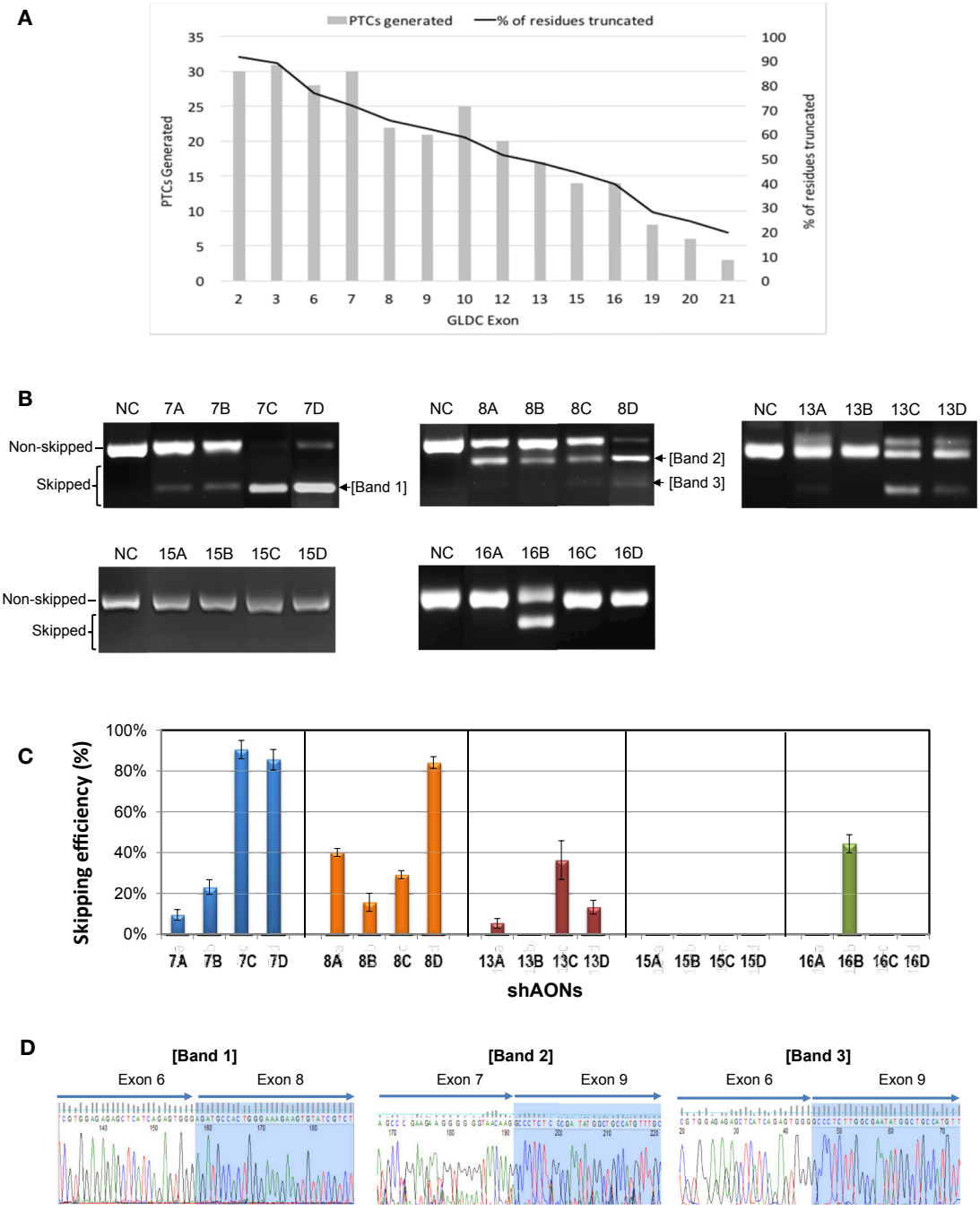

Figure 1. Transfection of shAONs at 100 nM Leads to Efficient and Specific Skipping of GLDC Target Exon in A549 Cells

(A) The number of PTCs generated and the percentage of amino acid residues removed when each of the 14 out-of-frame exons are skipped individually. GLDC has a total of 25 exons. (B) Images of agarose gel electrophoresis of the PCR products demonstrating specific exon skipping induced by shAON transfection in A549 cells. Cells were harvested 24 hr post-transfection. 100 μg/mL cycloheximide was added 5 hr after shAON transfection to inhibit the skipped transcripts from undergoing NMD. (C) The exon-skipping efficiency induced by each shAON as determined by densitometry analysis of the PCR products. The y axis shows the skipping efficiency, which is the percentage of the amplicons with exon skipping relative to the total amplicons (skipped + non-skipped). Data are presented as means ± SEM. (D) DNA sequencing of the bands corresponds to the skipped transcript excised from agarose gel (as indicated in B) to confirm skipping of the specific target exon.

Table 1. shAON Sequences

Target Exon	Label	shAON Sequences (5′ to 3′)
7	7A	AGG UGG CCU CAA GAU GCA CAA AGC UAA AAG G
	7B	AUU CUC CAG GUG GCC UCA AGA UGC ACA AAG
	7C	AAG CUA AAA GGU CAG UAG CAC AGC AGG CCA GG
	7D	AAG GUC AGU AGC ACA GCA GGC CAG GCU
8	8A	UUG UCU CUC CGA AUG UGU UGC UCC CUG GUU
	8B	UGU UGC UCC CUG GUU UGA AGA GCA AGA CG
	8C	GGU AGC CUU GUC UCU CCG AAU GUG UUG C
	8D	UCU CUC CGA AUG UGU UGC UCC CUG GUU UGA
13	13A	UGU GAA CAA GGG AAA UGU CUU UAU UUU C
	13B	UCA UGU ACC GGA CAA UGU UUG UUU CAG AGU GG
	13C	GUU UCU UCA UGU ACC GGA CAA UGU UUG UUU
	13D	AUG UCU UUA UUU UCC AGU UUC UUC AUG UA
15	15A	AUG UUU GCA AAU UCU UUC CAU GUG AUA GG
	15B	AGG GGU GGA UGU UUG CAA AUU CUU UCC AUG U
	15C	GGC ACA AAG GGG UGG AUG UUU GCA AA
	15D	UCC AGA GGC ACA AAG GGG UGG AUG UU
16	16A	UGG UUU AAG UAG GCU CGG AUA GUG GCC AGU CC
	16B	UUU CUG GUU UAA GUA GGC UCG GAU AGU G
	16C	UAG UGG CCA GUC CAG CAU AUU CUC CCU GGG
	16D	CUC GGA UAG UGG CCA GUC CAG CAU AUU C
–	NC	CCU UCC CUG AAG GUU CCU CC
	NC3	G CAG AUG AAC UUC AGG GUC AGC UUG

Each shAON was synthesized as RNA bases modified with 2′-O-methyl linked by phosphorothioate backbones (2OMePS). NC, scrambled sequence as the negative control.

The dose-dependent efficacy of the shAON for downregulation of GLDC protein level was determined by western blotting analysis at 72 hr after transfection. Notably, the IC_{50} for protein-level suppression is <10 nM for each of the three shAONs, with nearly complete depletion at 20 nM (Figure 2C).

shAONs Inhibit A549 Cell Growth and Proliferation and Tumorigenic Potential

To determine the effect of the candidate shAONs on cell growth and proliferation, we transfected A549 cells with shAONs 7C, 7D, or 8D at various concentrations, and cell viability was measured using 3-(4,5-dimethylthiazol-2-yl)-2,5-diphenyltetrazolium bromide (MTT) assay at 0, 24, 48, 72, and 120 hr after transfection. Three different negative controls were used for this experiment: (1) untransfected cells, (2) cells treated with transfection reagent (Lipofectamine 2000) alone, and (3) cells transfected with scrambled shAON (NC). A549 cell proliferation was suppressed by shAONs 7C, 7D, or 8D, which lasted for at least 5 days (120 hr) after transfection at 10 nM (Figure 3A). The extent of cell growth inhibition at 120 hr after transfection increased from 35% at 5 nM to almost 100% at 30 nM (Figure 3B). In contrast, cell viability of two non-cancer cell lines, HLF and MRC-5, was not reduced significantly when transfected with shAONs 7C, 7D, or 8D (Figure 3C).

As anchorage-independent growth correlates with tumorigenicity of transformed cells, A549 cells transfected with shAONs 7C, 7D, 8D, or NC were examined for their abilities to form colonies in soft agar. At 7 days after transfection, substantially fewer colonies were observed for cells treated with shAONs 7C, 7D, or 8D than those transfected with scrambled shAON (NC) at all concentrations used in this experiment (Figure 3D). Colony formation was inhibited almost entirely by shAONs 7C and 8D at transfection concentration of 30 nM. Together, these results demonstrate that our candidate shAONs are able to suppress the growth, proliferation, and anchorage-independent growth of A549 cells whose growth and survival are contingent upon high GLDC expression level. Because both untransformed HLF and MRC-5 cells are refractory to the shAON-mediated suppression of GLDC expression, these candidate shAONs may have a wide therapeutic index.

shAON-Mediated GLDC Knockdown in TIC-Enriched Lung Tumor Sphere Cells Inhibits Cell Growth and Proliferation and Tumorigenic Potential

It has been shown previously that tumor sphere TS32 cells are highly enriched in TICs (1 in 5,175 tumor cells; p = 1.37E−23).[6] In brief, freshly resected primary lung tumors from a NSCLC patient were directly transplanted subcutaneously into *NOD.Cg-Prkdc^{scid} Il2rg^{tm1Wjl}/SzJ* mice with Matrigel. NSCLC tumors excised from the mice were fractionated by FACS to isolate $CD166^+$ Lin^- cells. Lastly, the cells were cultured for sphere formation to select and further enrich for TICs, which expanded during the in vitro culturing to form tumor spheres. The increased tumor-initiating capacity of the tumor sphere cells suggests that they are more highly enriched for TICs than the patient tumor $CD166^+$ fraction and are 77× higher than in unsorted and unenriched primary samples.[35]

Tumor sphere TS32 cells were found to overexpress GLDC (Figure S1A). Based on the exon-skipping efficiency measured by densitometry (Figure 4A) and confirmed by real-time qPCR (Figure S1D), shAONs 7C, 7D, and 8D can each induce specific skipping of its respective target exon in GLDC transcripts in TS32 cells, with IC_{50} ranging from 65 to 220 nM. Consistent with the observations for A549 cells, both 7C and 7D exhibit greater exon-skipping efficiency than 8D. Similarly, GLDC protein level was also effectively reduced in TS32 tumor spheres by each of the shAONs when transfected at 200 nM (Figure 4B). Our observation that the effective concentration of shAON for TS32 cells is higher than that for adherent A549 cells is perhaps due to the higher expression level of GLDC in the former (Figure S1A), thus requiring a higher amount of shAONs to target more GLDC transcripts. This is not due to poor transfection efficiency in TS32 cells because in the absence of transfection agent (Lipofectamine), 100 nM concentration of shAON 7D was able to induce exon 7 skipping, GLDC downregulation, and TS32 cell growth inhibition at efficiencies of 55% (Figure S2A), 37% (Figure S2B), and

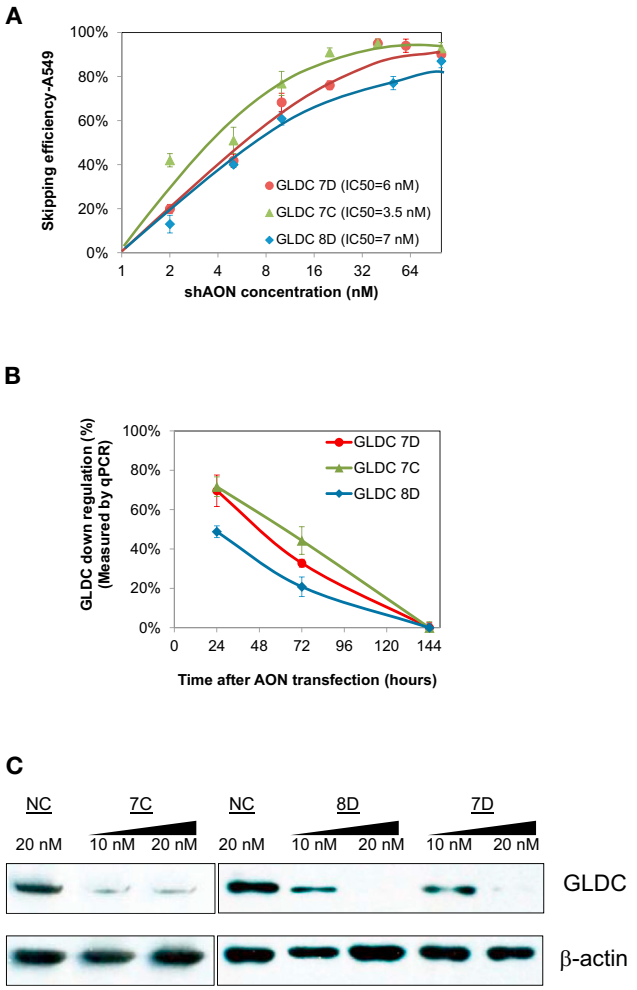

Figure 2. Dose Response of the Three Most Efficient shAONs

(A) Dose-response curves of shAON-induced exon-skipping efficiency (measured by densitometry analysis) in A549 cells. Cells were harvested 24 hr post-transfection. 100 μg/mL cycloheximide was added 5 hr after shAON transfection to inhibit the skipped transcripts from undergoing NMD. Data are presented as means ± SEM. (B) Time-course experiment showing the downregulation of GLDC transcript level (measured by real-time PCR) in A549 cells at different time points up to 144 hr post-transfection. Cycloheximide was not added in this experiment. Data are presented as means ± SEM. (C) Western blotting of GLDC protein with β-actin as loading control showing the dose effect of shAON. Protein extraction was performed 72 hr after transfection.

18% (Figure S2C), respectively. By comparison, no efficacy from shAON 7D was observed on A549 cells in the absence of transfection agent (Figure S2).

We also determined the effect of shAONs 7C, 7D, 8D, and NC (scrambled) on the growth and proliferation of the tumor sphere TS32 cells. Relative to the NC, the growth and proliferation of tumor sphere cells treated with 7C, 7D, or 8D was inhibited by 62%–76% at 150–250 nM concentrations (Figures 4C and 4D). In soft agar assay, treatment with 7C, 7D, or 8D (at transfection concentration of 200 nM) reduced colony formation in tumor sphere TS32 cells by 61%–76% (Figure 4E).

shAON 7D Inhibits Tumor Growth in Mice Grafted with Tumor Sphere TS32 Cells

Mice studies were performed to test the hypothesis that downregulation of GLDC inhibits tumor initiation. TIC-enriched TS32 tumour spheres were transplanted subcutaneously in 4 to 6 weeks old immune deficient mice (*NOD.Cg-Prkdc^{scid} Il2rg^{tm1Wjl}/SzJ* mice, 7-8 mice/treatment-group) at two distinct flanks (Materials and Methods). shAON 7D or NC (scrambled) was administered by intraperitoneal injection (50 mg/kg) at thrice/week dosing. To test the hypothesis that GLDC inhibition retards tumor initiation, we began the shAON administration on the day of implantation, which simulates the biological processes necessary for TIC to initiate tumor formation. The penetrance of the inhibition of tumor initiation in the mice was subsequently inferred from the inhibition of tumor growth relative to the control group. The mice were sacrificed after 6 weeks of treatment, and tumors from both flanks were extracted and weighed independently. The tumors from 7D- and NC-treated mice weighted with medians of 0.325 and 0.820 g, respectively, i.e., 60% inhibition of tumor growth ($p = 0.000676$ from unpaired t sample test or 0.00391 from unpaired Wilcoxon rank-sum test) (Figure 5A). RNA analysis of 20 tumor samples (12 and 8 from control and shAON 7D groups, respectively) showed that 7D treatment caused GLDC exon 7 or exons 7 and 8 (minor) skipping in all treated tumor samples, whereas almost no GLDC exon skipping was observed in NC-treated tumor samples (Figure 5B); extensive RNA degradation in the other nine tumor samples prevented RNA analysis. The correlation between exon-skipping efficiency and tumor weight, however, could not be determined because we were unable to measure the total amount of GLDC transcripts with skipped exon by PCR, required to calculate the exon-skipping efficiency. Because it is not possible to pre-treat the in vivo tumor cells with cycloheximide to inhibit nonsense-medicated decay (NMD), only GLDC transcripts that have not undergone or have yet to undergo NMD can be measured.

DISCUSSION

shAONs, synthesized entirely as RNA bases modified with either 2′-O-methyl or 2′-O-methoxyethyl, or as morpholino, and linked by phosphorothioate bonds, have been shown to be safe in independent human clinical trials.[19–21] Through competitive binding to sequence motifs utilized by splicing regulators, shAONs can modulate specific splicing events to correct the disrupted codon-reading frame or to induce mis-splicing events. These strategies have been applied typically to restore protein production in genetic diseases including Duchenne muscular dystrophy, spinal muscular atrophy, thalassemia, and cystic fibrosis.[19–22,36,37] Splice-modulating shAONs used in this study, on the other hand, are directed to disrupt the codon-reading frame and generate PTCs to induce NMD pathway for target degradation.[25,31] Interestingly, the consensus sequences at both the ribosome binding site and splice sites are conserved. Hence, potential off-targets of shAONs can be eliminated by avoiding the targeting of the ribosome binding site or splice sites flanking the exon to induce

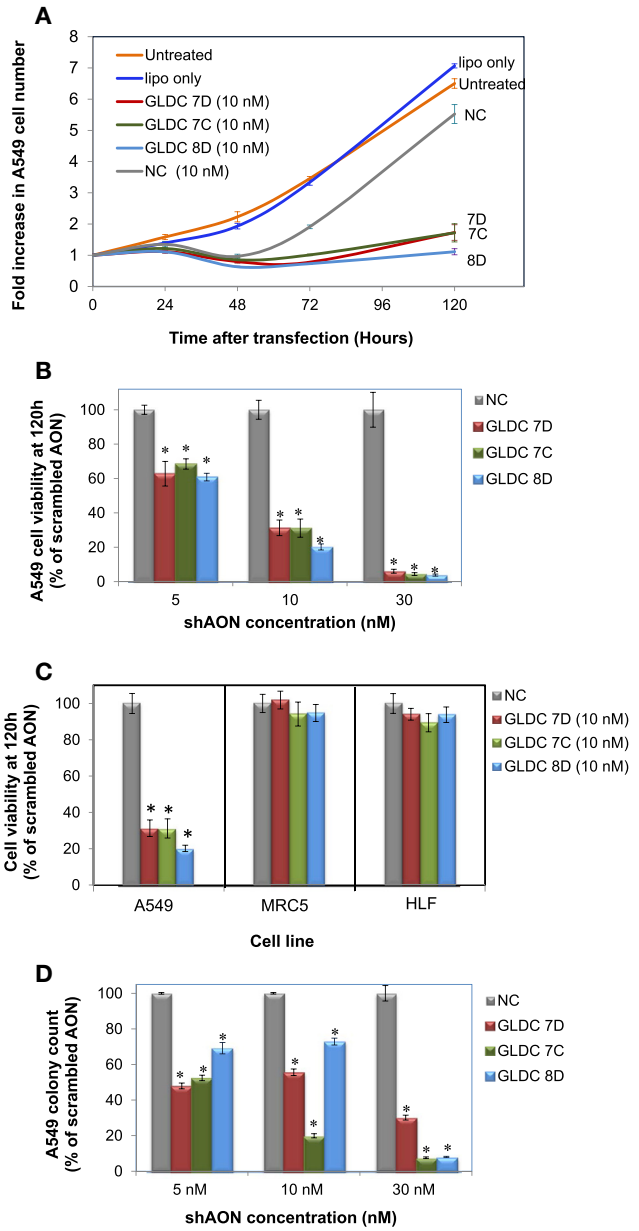

Figure 3. shAONs Inhibit A549 Cell Growth and Proliferation and Tumorigenesis

Data are presented as means ± SEM. (A) Growth curve of A549 cells after shAON transfection at 10 nM. (B) Effect of various concentrations of shAONs on A549 cell viability at 120 hr after transfection. (C) Comparison of cell viability between A549, MRC5, and HLF cells at 120 hr after transfected with shAONs 7C, 7D, or 8D at 10 nM. (D) Soft agar assay of A549 cells transfected with shAON. The number of colonies was counted 7 days after transfection and was normalized with respect to the NC. Asterisks indicate that the results are significantly different (*$p < 0.01$, Student's t test) from the scrambled AON control in (B)–(D). lipo only, Lipofectamine 2000 only; NC, scrambled shAON.

exon skipping (Table 1). Use of shAONs provides some advantages over gapmers. Unlike gapmers, shAONs can also mitigate non-specific binding to the human transcriptome. Every ribonucleic base within an shAON can be either modified chemically or substituted with a nucleotide mimetic to avoid non-complementary base-pair bindings. Similar chemical modification on every deoxyribonucleic base in a gapmer, however, will abolish its ability to activate RNase-H. In an event of partial complementary binding to the transcriptome, an shAON will result in off-target effects only when its binding site possesses motifs that are critical for the regulation or processing of a nascent transcript. By contrast, a gapmer induces degradation of any nascent and mature transcripts that it binds to, whether via non- or partial complementary base-pairing.

Keeping these advantages in view, we have identified in this study three efficacious splice-modulating shAONs candidates for the suppression of GLDC expression (Figure 1). shAONs 7C and 7D each induce exon 7 skipping, whereas 8D targets exon 8. Although these shAONs are designed to induce GLDC transcript degradation via the NMD pathway, any skipped transcripts if translated will produce a substantially truncated and non-functional protein (Figure 1A). Skipping of exon 7 generates 30 PTCs resulting in 71.9% truncation of the protein (287 amino acid residues remaining out of 1,021 residues), whereas skipping of exon 8 generates 22 PTCs resulting in 65.5% truncation (352 residues remaining). In both cases, the resultant protein is expected to lose the domains for glycine dehydrogenase activity, amino acid transport, and metabolic functions.[38]

In A549 cells, the IC_{50} attained by each candidate shAON lies between 3.5 and 7 nM for the induction of exon skipping and <10 nM for the downregulation of the expression of the GLDC protein (Figure 2). Notably, 7C achieves IC_{90} of 20 nM and <10 nM for exon exclusion and protein suppression, respectively. In primary NSCLC tumor spheres TS32 cells enriched with TICs (Figures 4A and 4B), IC_{50} for 7C, 7D, and 8D for the induction of exon skipping is 130, 65, and 220 nM, respectively. GLDC protein expression was almost completely suppressed by each shAON at 200 nM. In cell viability assays, A549 cell growth and proliferation was almost entirely halted by each candidate at 30 nM (Figures 3A and 3B), while in tumor sphere cells, the inhibition was 62% and 76% at 150 and 250 nM concentrations, respectively (Figures 4C and 4D). In contrast, no significant inhibition was observed in non-cancer MRC5 and HLF cells (Figure 3C). These results indicate that these candidate shAONs may exhibit good therapeutic index, as a consequence of tumor cells' dependence on the overexpression of GLDC for their proliferation and tumorigenesis. Colony formation on soft agar culture by A549 cells, which correlates with tumorigenicity, was almost completely abolished by 7C or 8D at 30 nM (Figure 3D), whereas the colony-forming capacity of tumor sphere cells TS32 was reduced by 61%–76% by the three candidate shAONs at 200 nM (Figure 4E). That a higher effective concentration of shAON is required for non-adherent tumor sphere cells is likely due to the higher expression level of GLDC in these cells (Figure S1A). Although cells with higher GLDC expression levels would typically require a higher dose of RNA therapeutic

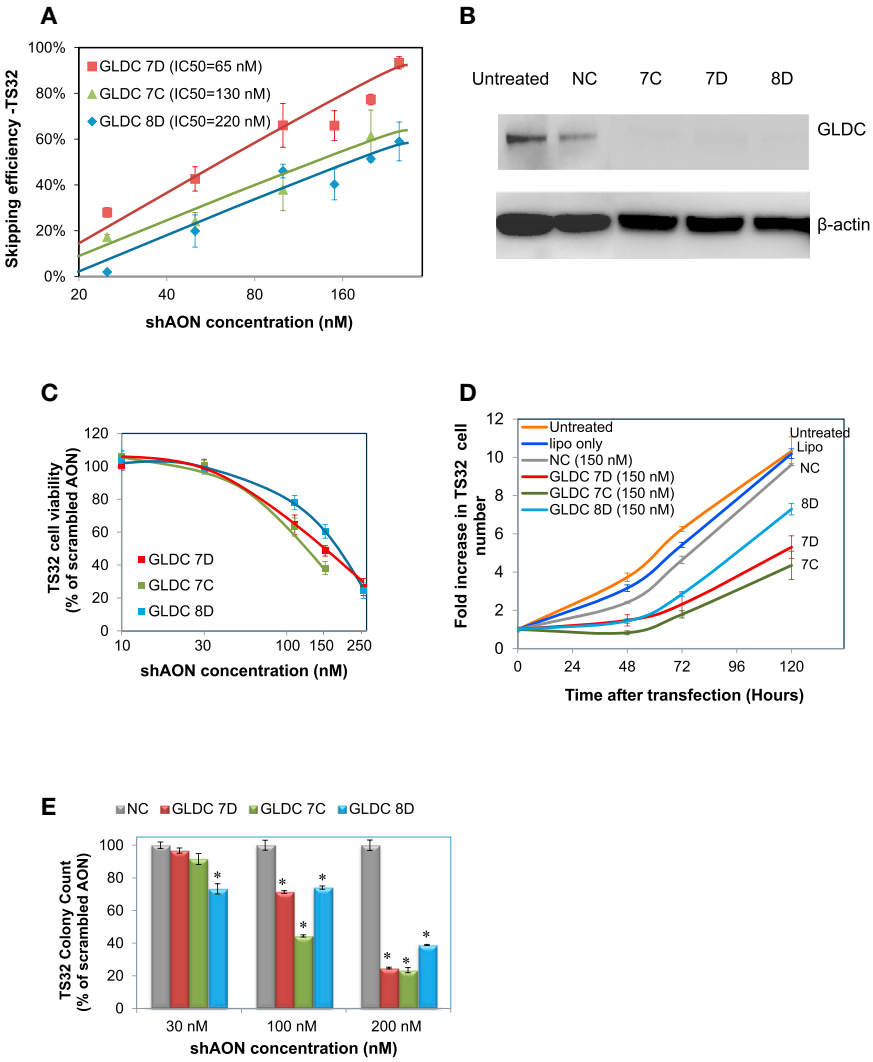

Figure 4. shAON-induced GLDC Knockdown Inhibits Cell Growth and Proliferation and Tumorigenesis of Lung Tumor Sphere TS32 Cells

Data are presented as means ± SEM. (A) Dose-response curves of shAON-induced exon-skipping efficiency in tumor sphere cells (measured by densitometry analysis). Cells were harvested 24 hr post-transfection. 100 μg/mL cycloheximide was added 5 hr after shAON transfection to inhibit the skipped transcripts from undergoing NMD. (B) Western blotting of GLDC protein (200 nM) in tumor sphere cells (72 hr after transfection) with β-actin as loading control. (C) shAON dose response measured using cell viability assay at 72 hr after transfection. (D) Growth curve of tumor spheres cells transfected with 150 nM shAONs. (E) Soft agar assay for tumor sphere cells transfected with shAON. The number of colonies was counted 7 days after transfection and was normalized with respect to NC samples. Asterisks indicate that the results are significantly different (*$p < 0.01$, Student's t test) from the scrambled AON control.

drug, this difficulty can be potentially mitigated when a drug candidate exhibits wide therapeutic index. Furthermore, our therapeutic strategy to target the pre-mRNA could be more effective in suppressing a target that is overexpressed. This is because targeting the pre-mRNA eliminates the amplification step of protein translation in which one mRNA serves as a template to produce multiple copies of the target protein. Lastly, shAON 7D reduced tumor growth by 60% in mice transplanted with the tumor sphere cells. The tumor growth inhibition in the 7D-treated group is likely due to the suppression of GLDC, given that exon 7 skipping was observed in all 7D-treated tumor samples, but almost none in the NC-treated samples (Figure 5B). Importantly, the mouse studies show that systemic delivery of 7D to tumor cells is effective without any further chemical modification or the use of a delivery agent.

The 60% inhibition of tumor growth by shAON 7D in mice transplanted with TS32 cells could be aided by two factors. First, we have shown that TS32 cells are amenable to acquire shAONs without a transfection reagent in cell cultures; it is possible that TS32 cells transplanted in mice behave in a similar manner. Second, the mean terminal half-life of 2′-O-methyl phosphorothioate chemistries of the shAONs used in this study is reported to be ~29 days in human plasma.[39] It is likely that repeated dosing in our mouse studies results in shAON accumulation and augments the inhibition of tumor growth, as reflected in the in vitro cultures of TS32 cells (Figure S2C). The fact that the length of the scrambled control shAON (NC) used in our study is shorter than the exon-targeting shAONs might have influenced the quantitative interpretation of the exon-targeting shAONs efficacy we have observed. To eliminate this possibility, we tested two additional controls, namely, NC3 and 15B, against our most effective shAONs (Table 1). As shown in Figure S2D, the effect of NC3 (which is a scrambled shAON with identical length as shAON 7D) on A549 and TS32 cell viability is almost identical to NC. On the other hand, 15B, an ineffective shAON targeting GLDC exon 15, reduces A549 cell viability by 10% more than NC. Therefore, the length of NC does not seem to influence, at least in vitro, its validity as a negative control.

Serine and glycine are necessary precursors for both protein synthesis and nucleotide metabolism crucial for the growth of cancer cells. Aberrant serine-glycine metabolism has become an emerging hallmark of a variety of cancers. In a recent study,[40] 60 primary human cancer cell lines from nine prevalent tumor types were analyzed, and the increased glycine consumption in rapidly proliferating cancer cells was found to be associated with high expression levels of the

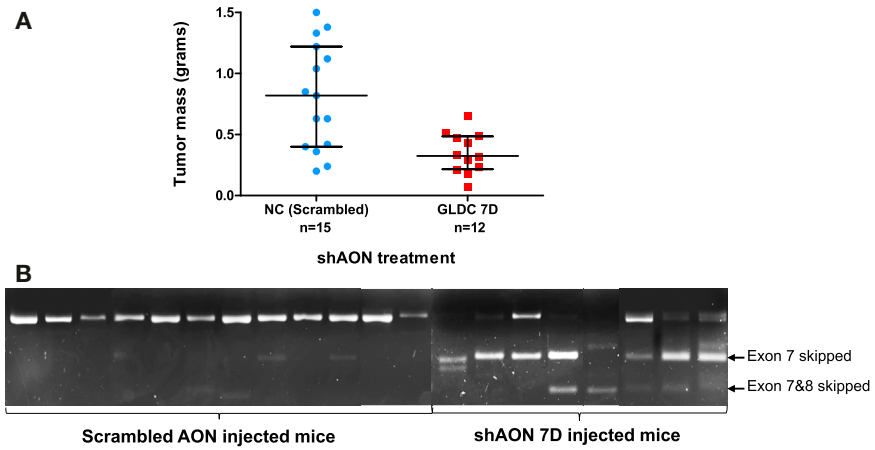

Figure 5. shAON 7D Inhibits Tumor Growth In Vivo

(A) Dot plot comparing tumor mass from mice treated with either shAON 7D or NC (Scrambled) (seven to eight mice/treatment group). Medians with error bars showing the 25th and 75th percentiles are indicated. The median mass of tumors from 7D-treated mice is 60% smaller than from NC-treated mice; p = 0.000676 (unpaired t sample test) and 0.00391 (unpaired Wilcoxon rank sum test). n represents the number of tumors in each group. (B) Gel electrophoresis analysis showing exon 7 skipping induced by shAON 7D compared with NC in 20 tumor samples (12 from scrambled control group, 8 from shAON 7D group) extracted from mice. Samples with no detectable PCR products due to RNA degradation are not included in the gel photo.

enzymes involved in the mitochondrial glycine-serine pathway. Multiple independent studies have reported the association between the overexpressions of the serine-glycine pathway enzymes with shorter survival times in patients with breast cancers,[7] phyllodes tumors,[8] and thyroid cancers.[9] Importantly, it is the mitochondrial pathway of the serine-glycine metabolic network, and not the cytosolic counterpart, that exhibits a significant correlation with cell proliferation. This suggests a key role for the mitochondria in supporting the rapid proliferation of cancer cells. The dependence on GLDC for tumorigenesis was further demonstrated in NSCLC TICs,[6] wherein the levels of GLDC expression were found to be significantly higher than in normal lung cells (Figure S1A). GLDC overexpression also leads to tumor formation in vivo, and knockdown of GLDC significantly reduces tumorigenicity of cancer cells.[6] Together, these observations justify GLDC as a relevant target for anticancer therapy.

The therapeutic value of GLDC may also be relevant to other forms of cancers. For instance, GLDC overexpression levels in acute leukemia cell lines, RS4;11 and THP-1, which harbor specific *MLL1* fusion translocation, are substantially higher than in A549 cells (Figure S1A) with GLDC expressions in RS4;11 and THP-1 cells 15- and 2-fold higher than that in A549 cells, respectively. The efficacy of shAONs 7C and 7D in inducing specific exon skipping in RS4;11 and THP-1 cells is similar to those in A549 and primary NSCLC tumor sphere cells (Figure S1E). In addition to GLDC, other components of the glycine synthesis pathway, such as phosphoserine aminotransferase 1 (PSAT) and serine hydroxyl methyl transferase 2 (SHMT2), may also be de-regulated. Hence, targeting of other nodes in the pathway singly or in combination may further delay or inhibit tumor growth in vivo. As shown in this study for GLDC, shAON-mediated exon skipping can be used to downregulate and/or eliminate the expression of other metabolic enzymes or proteins involved in the initiation and maintenance of various tumor types.

MATERIALS AND METHODS

All reagents were purchased from Sigma-Aldrich (Singapore) unless otherwise specified.

Cell Culture

Human lung adenocarcinoma epithelial cell line A549 was maintained in DMEM media supplemented with 10% FBS, 2 mM L-glutamine, and 1% penicillin-streptomycin (GIBCO, Thermo Fisher Scientific, Singapore). Normal human fetal lung fibroblast MRC-5 cells and human adult lung fibroblasts HLF cells were maintained in DMEM media supplemented with 10% FBS and 1% penicillin-streptomycin.

Tumor Sphere Culture

Tumor sphere TS32 cells were prepared from a NSCLC patient as previously described[6] and maintained in DMEM/F12 containing insulin-transferrin-selenium (ITS) supplement and supplemented with 0.4% BSA, 20 ng/mL epidermal growth factor (EGF), 4 ng/mL basic fibroblast growth factor (bFGF) (Invitrogen Singapore, Singapore), and 1% penicillin-streptomycin in non-treated Petri dish (Corning; Sigma-Aldrich, Singapore). Fresh medium was replenished every 3 days. Cells were split with Accutase (Merck Millipore, Singapore) to obtain single-cell suspensions.

shAON Design and Synthesis

All shAONs were rationally designed as previously described[32,33] and synthesized as RNA bases modified with 2′-O-methyl of phosphorothioate backbone (2OMePS) by Sigma-Aldrich (Singapore) and Integrated DNA Technology (Singapore). An shAON with a scrambled sequence was included in all experiments. shAONs used in mice experiments were purified by high performance liquid chromatography (HPLC) and were treated to remove endotoxins.

Cell Transfection with shAONs

Growth medium without antibiotics (i.e., penicillin-streptomycin) was used as transfection medium during cell transfection for all cells/cell lines. A549 cells were seeded in six-well plates at 1.0–1.5 × 10^5 cells/well in 1 mL transfection medium and were incubated for overnight. Cells reached around 40% confluence, and the culture medium was reduced to 900 μL before transfection. 10× Transfection mixture with a fixed ratio of 1:2 of shAON (in 100 pmol)/Lipofectamine 2000 (in μL) at various concentrations was prepared in Opti-MEM medium

(Invitrogen Singapore, Singapore) to a total volume of 100 μL, incubated for 20 min at room temperature, and added into the cell culture.

TS32 cells were seeded in 24-well plates at 1.0–1.5 × 10^5 cells/well in 900 μL of transfection medium. 10× Transfection mixture with various amounts of shAON and a fixed amount of Lipofectamine 2000 (5 μL) was prepared in Opti-MEM medium to a total volume of 100 μL, incubated for 20 min at room temperature, and added to the cell culture immediately following cell seeding.

For transfection experiment to measure shAON-induced exon skipping efficiency, cycloheximide was added in the cell medium (100 μg/mL) 5 hr after transfection to stop protein synthesis and RNA degradation mediated by the NMD pathway. However, no cycloheximide was added for transfection experiment to measure the effect of shAON on downregulation of GLDC transcript or cell viability and/or proliferation.

Quantification of shAON-Induced Exon-Skipping Efficiency and GLDC Transcripts Downregulation

24 hr after transfection with shAONs, cells were harvested and total RNA was extracted using QIAGEN RNeasy Mini Kit (QIAGEN Singapore, Singapore), treated with DNase (Ambion Turbo DNA-Free kit; Thermo Fisher Scientific, Singapore) to remove contaminating DNA, and transcribed into cDNA using SuperScript III Reverse Transcriptase (Invitrogen Singapore, Singapore) with random hexamer according to manufacturers' instructions.

For measurement of shAON-induced exon-skipping efficiency, PCRs were performed with primers amplifying the region covering the target exon and at least one neighboring exon on both sides. The PCR products were then verified by agarose gel electrophoresis and DNA sequencing to confirm skipping of the specific target exon. Exon-skipping efficiency was estimated by densitometry analysis of the gel images by calculating the amount of the targeted exon skip product relative to the total products (skipped transcript + non-skipped transcript). Densitometry analysis was performed using ImageJ software (W.S. Rasband, ImageJ; NIH, Bethesda, MD, USA).

Skipping efficiency was also measured indirectly using real-time qPCR with one primer (of a primer set) located within the targeted exon and the other primer outside the targeted exon to measure the amount of target exon-containing GLDC transcript using GADPH as endogenous reference in the corresponding samples and relative to the cells transfected with the same concentration of a scrambled shAON. Similarly, real-time qPCR was also performed to measure downregulation of GLDC transcript with forward primer located within exon 1 and reverse primer located within exon 3, and the data were normalized with GAPDH and compared with the corresponding scrambled shAON-transfected cells.

Cell Viability Assay

Measurement of cell viability and proliferation was performed in 96-well plate (3.5 × 10^3 cells in 100 μL medium per well) using the Thiazolyl Blue Tetrazolium Bromide (MTT) assay or CellTiter-Blue cell viability assay (Promega, Singapore). Cells were transfected in the 96-well plate with a mixture of shAON and Lipofectamine 2000. For MTT assay (used for adherent cells), medium was replaced by DMEM media (100 μL/well) with MTT (0.5 mg/mL) and incubated for 4 hr at 37°C, and then changed to 100 μL of isopropanol. Absorbance was measured using a microplate reader (Molecular Devices, Sunnyvale, CA, USA) at a wavelength of 570 nm with background subtraction at 630 nm and converted to the number of live cells using a calibration curve for absorbance against live cell number. For CellTiter-Blue cell viability assay (for suspension cells), Cell-Titer Blue reagent was added (11 μL/well) and incubated for 4 hr at 37°C. Fluorescence was measured using the microplate reader with an excitation of 570 nm and an emission of 600 nm.

Soft Agar Assay

24 hr following shAON transfection, cells were harvested, re-suspended with 0.4% of noble agar in DMEM medium, and plated onto 96-well plate (5 × 10^3 cells/well) containing a solidified bottom layer (0.6% noble agar in DMEM medium). Each well was covered with 100 μL of growth medium and incubated under standard culture conditions for 1 week. Cells were stained with CellTiter Blue, and colony counting was performed using a fluorescence microplate reader.

Western Blotting

Proteins were extracted from cells using mammalian protein extraction reagent (M-PER) lysis buffer containing Halt protease inhibitor cocktail (Thermo Fisher Scientific, Singapore) with gentle shaking for 10 min at 4°C. Cell debris was removed by centrifugation at 12,000 relative centrifugal force (rcf) for 20 min at 4°C, and protein concentration of the supernatant was measured using Bio-Rad protein assay according to manufacturer's instruction. 16 μg of protein from each sample was loaded on an 8% Bis-Tris SDS-PAGE gel (Bio-Rad, Singapore) prepared according to manufacturer's instructions, and samples were then transferred to a Bio-Rad nitrocellulose membrane. After blocking with 5% milk in phosphate buffer saline with tween-20 (PBST) for 1 hr, the membrane was incubated with polyclonal rabbit anti-human GLDC antibody (1:2,000; Abcam, UK) in 3% milk/PBST at 4°C for overnight, followed by incubation with Amersham horseradish peroxidase-conjugated anti-rabbit IgG (1:4,000) (GE Healthcare, Singapore) in 3% milk/PBST for 3 hr at room temperature. β-Actin was used as loading control for western blotting and mouse anti-human β-actin antibody (1:1,000) and horseradish peroxidase-conjugated anti-mouse IgG (1:4,000) were used as 1st and 2nd antibodies, respectively. Visualization was achieved by the enhanced chemiluminescence (ECL) system using the SuperSignal West Pico chemiluminescent substrate (Thermo Fisher Scientific, Singapore).

Data Analysis for In Vitro Experiments

All in vitro transfection experiments were done in triplicate to ensure reproducibility, and the results shown in the figures are representative of three individual transfection experiments. Statistical analysis was performed in GraphPad Prism (Version 5.01).

Animal Studies

All animal studies were approved by the Institutional Review Committee. *NOD.Cg-Prkdc^{scid} Il2rg^{tm1Wjl}/SzJ* mice (Jackson Laboratories) (7–8 mice/treatment group) at 4–6 weeks old were subcutaneously transplanted at two distinct flanks (250,000 cells/flank) with single-cell suspensions of tumor spheres in serum-free medium and Matrigel (1:1) (BD Biosciences, Singapore). 50 mg/kg dose of shAON was injected intraperitoneally three times per week. Mice were sacrificed after 6 weeks of injection protocol, and the tumor from each flank was extracted and weighed. Two independent experiments were performed: one study included 5 mice (3 shAON treated, 2 scrambled control treated) and another study included 10 mice (4 shAON treated, 6 scrambled control treated). In each study, the mice were obtained from a new litter, the shAONs (7D and scrambled control) were freshly synthesized, and a fresh sample of TS32 tumor sphere cells was used for transplantation. The mice study was designed to eliminate response biases between litters. Hence, instead of consigning all mice in a litter to the same treatment group, we randomly assigned littermates to either treatment group. The number of mice in each group for each trial is thus dependent on the litter size.

29 tumors were obtained from a total of 15 mice used in the two experiments; one of the flanks from a mouse in the scrambled control group failed to grow a tumor. From the tumor mass measurements, outliers were removed by standard statistical procedure: data points that lie outside the interval (first quartile minus 1.5 times of the interquartile range, third quartile plus 1.5 times of the interquartile range); 2 (from the shAON 7D-treated tumors) out of 29 data points were identified as outliers. The statistical tests were performed in R (Version 3.2.2) with the following null hypothesis: no effect on the mass of the tumors from mice treated with either scrambled or GLDC-targeting shAONs. An alternate hypothesis was as follows: the median mass of tumors from mice treated with GLDC-targeting shAON is smaller than from scrambled shAON-treated mice. The dot plot was done in GraphPad Prism (Version 5.01).

For RNA analysis, after cell disruption using 0.5 mm glass beads in Micro Smash MS-100 (3 × 45 s at 4,500 rpm) (TOMY Digital Biology, Japan), total RNAs were extracted from tumor samples using QIAGEN RNeasy Mini Kit, reverse-transcribed to cDNA, and analyzed by PCR measurement of shAON-induced exon-skipping efficiency.

SUPPLEMENTAL INFORMATION

Supplemental Information includes two figures and can be found with this article online at https://doi.org/10.1016/j.omtn.2017.10.001.

AUTHOR CONTRIBUTIONS

J.L., Z.W., Z.A.D.P., B.L., K.B.W., and U.S. conceived and designed the experiments. K.B.W. designed the shAONs. J.L., J.H.J.L., K.P., and E.P. performed the experiments. J.L. and K.B.W. analyzed the data. J.L., K.B.W., and U.S. wrote the paper.

CONFLICTS OF INTEREST

A Patent Cooperation Treaty (PCT) application entitled "Steric hindrance antisense oligonucleotides (shAONs) targeting glycine decarboxylase (GLDC) expression as drug candidates for NSCLC and other cancers" has been filed (Application No. 10201609048R, Priority date: October 28, 2016).

ACKNOWLEDGMENTS

This work was supported by Agency for Science, Technology and Research (A*STAR), Singapore. K.B.W. and U.S. acknowledge support from JCO-ASTAR (grant 1231BFG043). K.B.W. acknowledges support from an IHPC Independent Investigatorship. Z.W. acknowledges support from the National Medical Research Council (grant NMRC/TCR/007-NCC/2013).

REFERENCES

1. Zhou, B.B.S., Zhang, H., Damelin, M., Geles, K.G., Grindley, J.C., and Dirks, P.B. (2009). Tumour-initiating cells: challenges and opportunities for anticancer drug discovery. Nat. Rev. Drug Discov. *8*, 806–823.
2. Vidal, S.J., Rodriguez-Bravo, V., Galsky, M., Cordon-Cardo, C., and Domingo-Domenech, J. (2014). Targeting cancer stem cells to suppress acquired chemotherapy resistance. Oncogene *33*, 4451–4463.
3. Garvalov, B.K., and Acker, T. (2011). Cancer stem cells: a new framework for the design of tumor therapies. J. Mol. Med. (Berl.) *89*, 95–107.
4. DeBerardinis, R.J., and Chandel, N.S. (2016). Fundamentals of cancer metabolism. Sci. Adv. *2*, e1600200.
5. Amelio, I., Cutruzzolá, F., Antonov, A., Agostini, M., and Melino, G. (2014). Serine and glycine metabolism in cancer. Trends Biochem. Sci. *39*, 191–198.
6. Zhang, W.C., Shyh-Chang, N., Yang, H., Rai, A., Umashankar, S., Ma, S., Soh, B.S., Sun, L.L., Tai, B.C., Nga, M.E., et al. (2012). Glycine decarboxylase activity drives non-small cell lung cancer tumor-initiating cells and tumorigenesis. Cell *148*, 259–272.
7. Kim, S.K., Jung, W.H., and Koo, J.S. (2014). Differential expression of enzymes associated with serine/glycine metabolism in different breast cancer subtypes. PLoS ONE *9*, e101004.
8. Kwon, J.E., Kim, D.H., Jung, W.H., and Koo, J.S. (2014). Expression of serine and glycine-related enzymes in phyllodes tumor. Neoplasma *61*, 566–578.
9. Sun, W.Y., Kim, H.M., Jung, W.H., and Koo, J.S. (2016). Expression of serine/glycine metabolism-related proteins is different according to the thyroid cancer subtype. J. Transl. Med. *14*, 168.
10. Hopkins, A.L., and Groom, C.R. (2002). The druggable genome. Nat. Rev. Drug Discov. *1*, 727–730.
11. Dancey, J., and Sausville, E.A. (2003). Issues and progress with protein kinase inhibitors for cancer treatment. Nat. Rev. Drug Discov. *2*, 296–313.
12. Overington, J.P., Al-Lazikani, B., and Hopkins, A.L. (2006). How many drug targets are there? Nat. Rev. Drug Discov. *5*, 993–996.
13. Kole, R., Krainer, A.R., and Altman, S. (2012). RNA therapeutics: beyond RNA interference and antisense oligonucleotides. Nat. Rev. Drug Discov. *11*, 125–140.
14. Krieg, A.M. (2006). Therapeutic potential of Toll-like receptor 9 activation. Nat. Rev. Drug Discov. *5*, 471–484.
15. Bonetta, L. (2009). RNA-based therapeutics: ready for delivery? Cell *136*, 581–584.
16. Krieg, A.M. (2011). Is RNAi dead? Mol. Ther. *19*, 1001–1002.
17. Geary, R.S., Yu, R.Z., and Levin, A.A. (2007). Modified antisense oligonucleotides in animals and man. In Antisense Drug Technology: Principles, Strategies, and Applications, S.T. Crooke, ed. (CRC Press), pp. 183–217.
18. Couzin-Frankel, J. (2010). Drug research. Roche exits RNAi field, cuts 4800 jobs. Science *330*, 1163.

19. van Deutekom, J.C., Janson, A.A., Ginjaar, I.B., Frankhuizen, W.S., Aartsma-Rus, A., Bremmer-Bout, M., den Dunnen, J.T., Koop, K., van der Kooi, A.J., Goemans, N.M., et al. (2007). Local dystrophin restoration with antisense oligonucleotide PRO051. N. Engl. J. Med. *357*, 2677–2686.

20. Kinali, M., Arechavala-Gomeza, V., Feng, L., Cirak, S., Hunt, D., Adkin, C., Guglieri, M., Ashton, E., Abbs, S., Nihoyannopoulos, P., et al. (2009). Local restoration of dystrophin expression with the morpholino oligomer AVI-4658 in Duchenne muscular dystrophy: a single-blind, placebo-controlled, dose-escalation, proof-of-concept study. Lancet Neurol. *8*, 918–928.

21. Passini, M.A., Bu, J., Richards, A.M., Kinnecom, C., Sardi, S.P., Stanek, L.M., Hua, Y., Rigo, F., Matson, J., Hung, G., et al. (2011). Antisense oligonucleotides delivered to the mouse CNS ameliorate symptoms of severe spinal muscular atrophy. Sci. Transl. Med. *3*, 72ra18.

22. Pao, P.W., Wee, K.B., Yee, W.C., and Pramono, Z.A. (2014). Dual masking of specific negative splicing regulatory elements resulted in maximal exon 7 inclusion of SMN2 gene. Mol. Ther. *22*, 854–861.

23. Nomakuchi, T.T., Rigo, F., Aznarez, I., and Krainer, A.R. (2016). Antisense oligonucleotide-directed inhibition of nonsense-mediated mRNA decay. Nat. Biotechnol. *34*, 164–166.

24. Tallet-Lopez, B., Aldaz-Carroll, L., Chabas, S., Dausse, E., Staedel, C., and Toulmé, J.J. (2003). Antisense oligonucleotides targeted to the domain IIId of the hepatitis C virus IRES compete with 40S ribosomal subunit binding and prevent in vitro translation. Nucleic Acids Res. *31*, 734–742.

25. Kang, J.K., Malerba, A., Popplewell, L., Foster, K., and Dickson, G. (2011). Antisense-induced myostatin exon skipping leads to muscle hypertrophy in mice following octa-guanidine morpholino oligomer treatment. Mol. Ther. *19*, 159–164.

26. Koh, C.M., Bezzi, M., Low, D.H., Ang, W.X., Teo, S.X., Gay, F.P., Al-Haddawi, M., Tan, S.Y., Osato, M., Sabò, A., et al. (2015). MYC regulates the core pre-mRNA splicing machinery as an essential step in lymphomagenesis. Nature *523*, 96–100.

27. Toh, C.X.D., Chan, J.W., Chong, Z.S., Wang, H.F., Guo, H.C., Satapathy, S., Ma, D., Goh, G.Y., Khattar, E., Yang, L., et al. (2016). RNAi reveals phase-specific global regulators of human somatic cell reprogramming. Cell Rep. *15*, 2597–2607.

28. Duan, M., Zhou, Z., Lin, R.X., Yang, J., Xia, X.Z., and Wang, S.Q. (2008). In vitro and in vivo protection against the highly pathogenic H5N1 influenza virus by an antisense phosphorothioate oligonucleotide. Antivir. Ther. (Lond.) *13*, 109–114.

29. Gabriel, G., Nordmann, A., Stein, D.A., Iversen, P.L., and Klenk, H.D. (2008). Morpholino oligomers targeting the PB1 and NP genes enhance the survival of mice infected with highly pathogenic influenza A H7N7 virus. J. Gen. Virol. *89*, 939–948.

30. Zhang, T., Wang, T.C., Zhao, P.S., Liang, M., Gao, Y.W., Yang, S.T., Qin, C., Wang, C.Y., and Xia, X.Z. (2011). Antisense oligonucleotides targeting the RNA binding region of the NP gene inhibit replication of highly pathogenic avian influenza virus H5N1. Int. Immunopharmacol. *11*, 2057–2061.

31. Holbrook, J.A., Neu-Yilik, G., Hentze, M.W., and Kulozik, A.E. (2004). Nonsense-mediated decay approaches the clinic. Nat. Genet. *36*, 801–808.

32. Pramono, Z.A.D., Wee, K.B., Wang, J.L., Chen, Y.J., Xiong, Q.B., Lai, P.S., and Yee, W.C. (2012). A prospective study in the rational design of efficient antisense oligonucleotides for exon skipping in the DMD gene. Hum. Gene Ther. *23*, 781–790.

33. Wee, K.B., Pramono, Z.A., Wang, J.L., MacDorman, K.F., Lai, P.S., and Yee, W.C. (2008). Dynamics of co-transcriptional pre-mRNA folding influences the induction of dystrophin exon skipping by antisense oligonucleotides. PLoS ONE *3*, e1844.

34. Fairbrother, W.G., Yeh, R.F., Sharp, P.A., and Burge, C.B. (2002). Predictive identification of exonic splicing enhancers in human genes. Science *297*, 1007–1013.

35. Ishizawa, K., Rasheed, Z.A., Karisch, R., Wang, Q., Kowalski, J., Susky, E., Pereira, K., Karamboulas, C., Moghal, N., Rajeshkumar, N.V., et al. (2010). Tumor-initiating cells are rare in many human tumors. Cell Stem Cell *7*, 279–282.

36. Xie, S.Y., Li, W., Ren, Z.R., Huang, S.Z., Zeng, F., and Zeng, Y.T. (2011). Correction of β654-thalassaemia mice using direct intravenous injection of siRNA and antisense RNA vectors. Int. J. Hematol. *93*, 301–310.

37. Nissim-Rafinia, M., Linde, L., and Kerem, B. (2006). The CFTR gene: structure, mutations, and specific therapeutic approaches. In Cystic Fibrosis in the 21st Century, Volume 34, A. Bush, E.W.F.W. Alton, J.C. Davies, U. Griesenbach, and A. Jaffe, eds. (Karger), pp. 2–10.

38. Marchler-Bauer, A., Derbyshire, M.K., Gonzales, N.R., Lu, S., Chitsaz, F., Geer, L.Y., Geer, R.C., He, J., Gwadz, M., Hurwitz, D.I., et al. (2015). CDD: NCBI's conserved domain database. Nucleic Acids Res. *43*, D222–D226.

39. Goemans, N.M., Tulinius, M., van den Akker, J.T., Burm, B.E., Ekhart, P.F., Heuvelmans, N., Holling, T., Janson, A.A., Platenburg, G.J., Sipkens, J.A., et al. (2011). Systemic administration of PRO051 in Duchenne's muscular dystrophy. N. Engl. J. Med. *364*, 1513–1522.

40. Jain, M., Nilsson, R., Sharma, S., Madhusudhan, N., Kitami, T., Souza, A.L., Kafri, R., Kirschner, M.W., Clish, C.B., and Mootha, V.K. (2012). Metabolite profiling identifies a key role for glycine in rapid cancer cell proliferation. Science *336*, 1040–1044.